



Experimental study of a novel layer deposition technique and its effect on anisotropic behavior of wire arc additively manufactured steel parts

Esraa S. Abdelall¹ · Abdullah F. Al-Dwairi¹ · Esraa Ashour¹ · Mohamed Eldakrouy²

Received: 13 September 2020 / Accepted: 15 June 2021 / Published online: 19 June 2021
© The Author(s), under exclusive licence to Springer Nature Switzerland AG 2021

Abstract

This work investigates the possibility of reducing the anisotropic behavior of wire arc additively manufactured (WAAM) parts by a new layer deposition technique. An experiment was carried out in which specimens were printed using AWS E6013 low carbon steel electrodes. In printing the specimens, sets of layers were deposited bottom-up (along Z-axis) at different inclination angles (namely, 0° , $\pm 15^\circ$, $\pm 30^\circ$ and $\pm 45^\circ$) with respect to X-axis of substrate XZ-plane. Results show that the proposed technique does reduce anisotropic behavior of printed parts when deposition angles of $\pm 30^\circ$ and $\pm 45^\circ$ are used. Parts printed with layer sets deposited at $\pm 45^\circ$ inclinations showed least anisotropy and highest tensile strength, but they also had longer building times as compared with the other specimens.

Keywords Wire arc additive manufacturing · Anisotropy · Build orientation · Layer deposition angle · Tensile strength · Toughness

1 Introduction

Additive manufacturing (AM), which is also known as rapid prototyping, emerged in the late 1980s with the purpose to shorten product development process and to help designers make more creative designs. Tremendous efforts have been made to develop and improve the AM processes to make them more reliable. It is known that AM processes have certain general shortcomings including low productivity and the difficulty of making fully functional parts. This has limited

the use of AM processes to product prototyping purposes in most cases. Today, although better tolerances and finishes, as well as shorter processing times have become possible, printing a fully functional AM part remains difficult. Recently, great attention was directed toward building more functional parts wherein researchers tried to control the factors that affect part mechanical properties. Some hybrid (additive-subtractive) rapid processes are also being used to improve printed part functionality. However, the well-known anisotropic behavior of AM parts gained little attention in research although this behavior is known to limit part functionality. As the anisotropic behavior of AM parts is usually linked to build orientation (see [1–3]), this work was undertaken to investigate potential usefulness of changing layer deposition pattern as a means of reducing this anisotropic behavior. The experiments were conducted using wire arc additive manufacturing process (WAAM).

✉ Esraa S. Abdelall
abdallesra@gmail.com

Abdullah F. Al-Dwairi
dwairy@just.edu.jo

Esraa Ashour
es_ashour93@yahoo.com

Mohamed Eldakrouy
mdakrory@iastate.edu

¹ Industrial Engineering Department, Jordan University of Science and Technology, P.O.Box 3030, Irbid 22110, Jordan

² Department of Industrial and Manufacturing System Engineering, Iowa State University, 3004 Black Engineering, 2529 Union Drive, Ames, IA 50011, USA

2 Related work

As a common practice, improving the functionality of additively manufactured parts is approached by utilizing stronger materials such as metals. Therefore, most of the research has mainly focused on developing new processes to enable

the use of metals in AM. Processes include wire arc AM (WAAM), subtractive-based processes, and hybrid AM processes. Although these processes facilitate metal AM and hence allow building more functional parts ([4, 5]), full functionality of the parts, especially along the build direction, has remained unachievable. Basically, poor interlaminar mechanical properties and the associated anisotropic behavior are the main factors that complicate the production of fully functional parts [6]. Moreover, anisotropy is noticed in almost all of the mechanical properties regardless of the AM technique used. For example, tensile and compressive strengths, hardness, and fatigue strength were all found to be much lower in the build direction (Z-axis) than in the XY-plane [1–3].

Despite its significance, the build orientation factor and its effect on anisotropy has not been investigated sufficiently in the AM literature. The few works that were found in this area mainly study anisotropy resulting from microstructural variations and defects within individual layers. The works [7–11] showed that in general, the presence of columnar grains and dendritic structure, in addition to uncontrolled grain size, are the factors responsible for the asymmetrical mechanical behavior within individual layers, as well as throughout the parts. Other studies such as [12–14] investigated the effects of process-induced defects such as porosity, residual stresses and associated distortions, and poor surface finish. These studies showed that these defects contribute to anisotropy within individual layers. Different treatment methods therefore were used in these studies to help obtain more isotropic properties within layers. Some of the treatment methods were directed at controlling the AM process parameters such as welding speed, peak current, travel speed, wire feed speed, arc mode, and others. These studies linked microstructural variations and defects to poor process parameter control. Other treatments were based on post-deposition microstructure homogenization and included different traditional heat treatment ([15–18]), and post-process deformation such as high pressure inter-pass (HIP) rolling ([9, 10, 15, 19]), laser shock peening (LSP) [8], and switch-back technique [7]. Although those treatments were found effective in reducing anisotropy within layers, anisotropic behavior associated with poor interlaminar strength along the build direction remained dominant.

Besides, the works [20–26] studied the effect of rastering angles within XY-plane on the surface roughness, accuracy, tensile properties, ductility, and hardness of AM parts. Different rastering directions in XY-plane (0° , $\pm 45^\circ$, 90°) were tested and found to cause considerable anisotropic behavior in built parts [27–32]. The effect of build orientation on tensile strength, fatigue life, and reliability of AM parts was addressed in several works such as [33–37]. These works were limited to studying either the effect of rastering angles within XY plane ([33, 34]) or the effect of build orientation

(namely, horizontal, slanted at 45° , and vertical) while depositing all the layers parallel to each other ([35–37]). Similar to the rastering effect, these studies verified the fact that build orientation has significant effects on the fatigue life, tensile strength, and reliability of AM parts.

To summarize, the research effort in AM has focused on anisotropic behavior resulting either from microstructural variations within deposited layers (i.e. dendritic structure and columnar grains) or from processing defects. To our knowledge, no work has considered reducing the anisotropic behavior that is linked to weak interlaminar bonding. This work assumes that this kind of anisotropy can be reduced by changing the layer deposition pattern and proposes a new deposition technique for these purposes. The proposed technique has been tested using a WAAM process and is presented in the next sections.

3 Methodology

Traditionally, to build a part using WAAM, the wire is deposited on a substrate, layer by layer in bottom-up approach (Fig. 1a). Although multiple beads can be built beside each other to widen the layers (Fig. 1b), the build direction remains perpendicular to the deposition direction. In addition, the angle between the newly deposited layer and the layer underneath is Zero throughout the whole part. This building pattern is thought to be the main contributor to the weak interlaminar strength and anisotropic behavior of printed parts. In this work, we propose a new layer deposition technique in which sets of layers are deposited at different angles with respect to reference axis (X-axis) in

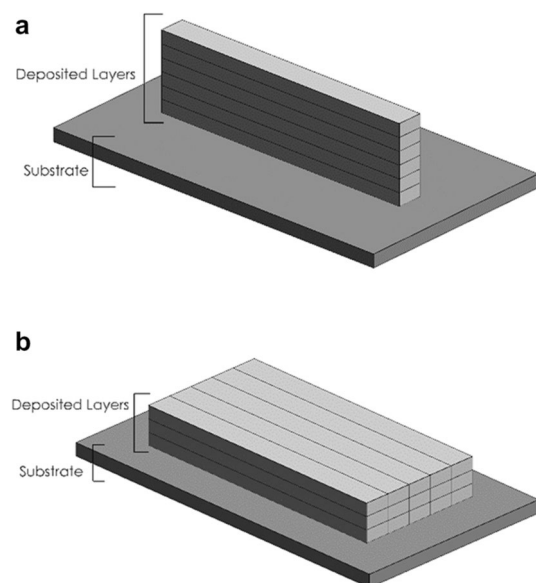


Fig. 1 Traditional deposition of layers

XZ-plane as shown in Fig. 2. An experiment was conducted using various deposition angles and electrode diameters, with the purpose to investigate the effect of this deposition technique on the printed part anisotropic behavior.

3.1 Description of the proposed deposition process

As illustrated in Fig. 2, to build a part using the proposed technique, the base plate (substrate) is first clamped to the machine bed using table flat bench and inclined at the required angle. Next, the process of adding metal layers starts while maintaining the deposition nozzle parallel to

z-axis and moving it along the x-axis (Fig. 2, Step 1). Passes are repeated until a set of layers has been deposited. The substrate is then rotated to the same angle in the opposite direction and a new set of layers is deposited (Fig. 2, Step 2). For example, if the starting angle is 15° counter-clockwise from the x-axis, then after depositing the first set of layers, the part will be rotated 15° clockwise from the x-axis. This process is repeated until the required build height is achieved (Fig. 2, Step 4). It is worth noting that, after each layer deposition, the layer surface is cleaned to remove any possible flux or grease that might weaken interlaminar bonding. Figure 3 shows sample photos taken during the preliminary testing in this work.

Fig. 2 Proposed deposition technique showing the sequence used to build test coupons

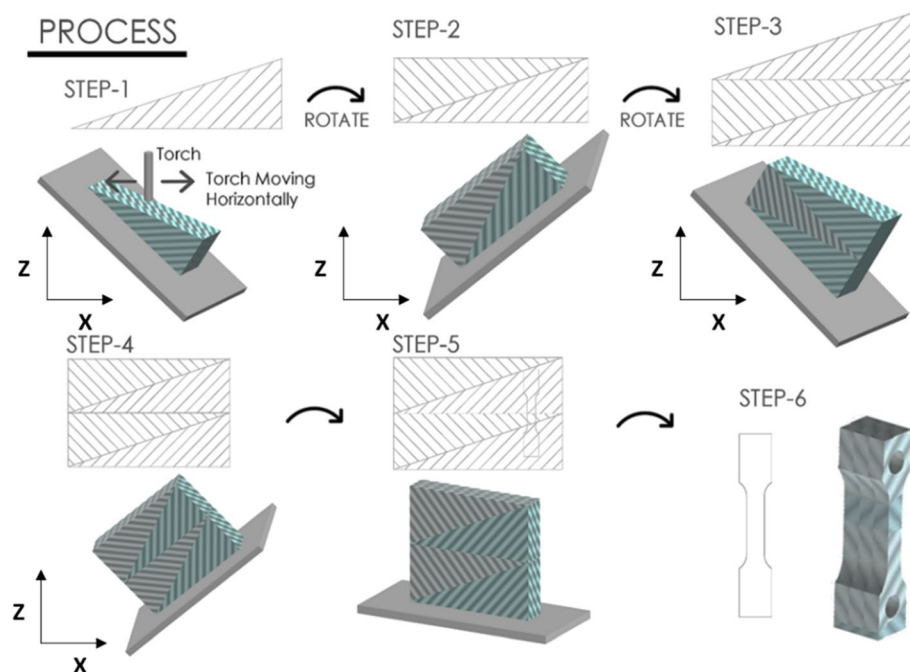


Fig. 3 Preliminary testing of the proposed deposition technique

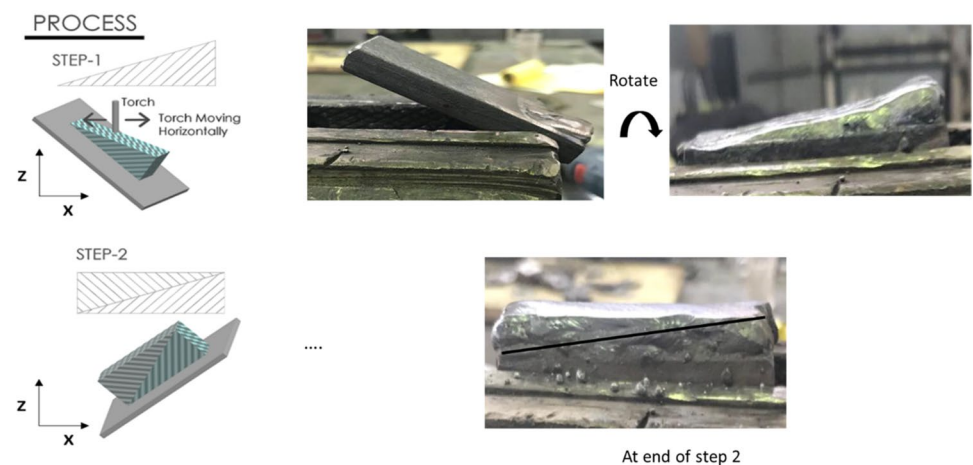


Table 1 Process factors and levels

Factor	Level			
Deposition angle	0°	15°	30°	45°
Electrode diameter	2.5 mm		3.2 mm	
Material: E6013				

Table 2 Chemical composition of wire (%)

C	Mn	Si	S	P	Fe
≤0.12	0.3–0.6	≤0.35	≤0.035	≤0.040	Balance

3.2 Experimental setting

In this work, shielded arc additive manufacturing (SAAM) as one of the WAAM processes was selected to test the proposed deposition technique. Table 1 summarizes the experiment design factors used to build the testing coupons. It should be noted that only four build angles were used in this work with a maximum build angle of 45°. The maximum build angle was limited to 45° because above this angle, interference between deposition electrode and build coupon was noticed during the preliminary tests.

The testing coupons were built using welding electrodes AWS E6013 made of low carbon steel. The chemical composition of the electrode material is provided in Table 2. The used substrate plate had dimensions 10×3×1 cm, while each coupon had dimensions 10×10×1 cm. The welding process was carried out using an AC/DC multi-function TIG welding machine with 122-A current.

The experiment was designed with four levels of the deposition angle factor and two levels of the electrode diameter factor. Three replicates were prepared from each combination of the factors hence a total of 24 coupons

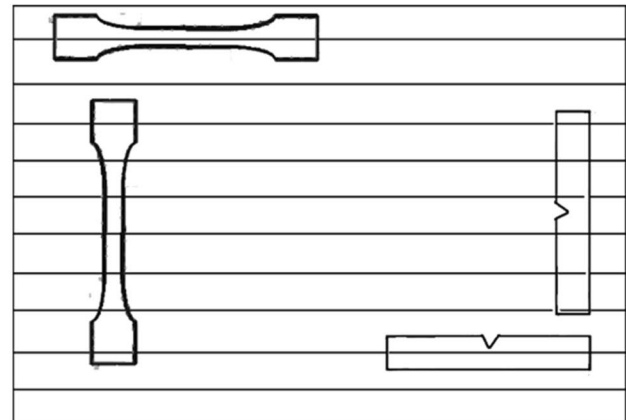
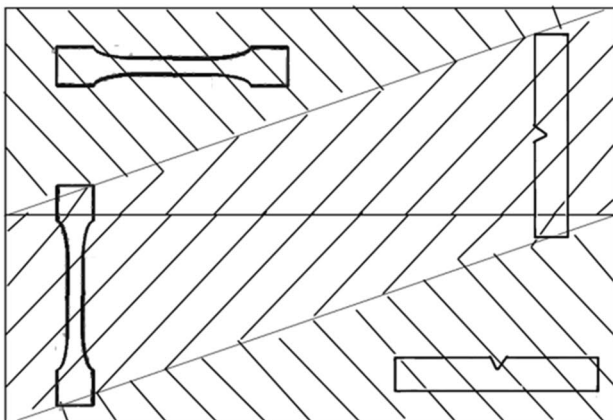
were prepared. Test samples cut from the coupons were tested for ultimate tensile strength (UTS) and toughness, in addition to examining their microstructure, fracture surface shape, and the numbers of beads/layers needed in each coupon. For the tensile tests, two samples were taken from each coupon: one in the transverse direction and another in the longitudinal direction (Fig. 4). The same was done for the impact test. Statistical analysis of the results was carried out using ANOVA.

3.3 Mechanical tests

Samples for tensile and toughness testing were cut using CNC machine along both longitudinal and transverse direction from each coupon, as illustrated in Fig. 4. Tensile samples were prepared according to ASTM D638 standard in a dog-bone-shaped rectangle with a gage length of 50 mm. The samples were fully annealed prior to testing. Tensile testing was then performed at room temperature by universal testing with speed of 1 mm/min. Toughness samples were prepared and tested according to ASTM D256 standard for Charpy test. Similar to tensile testing, all samples were also annealed prior to testing them at room temperature.

3.4 Fracture shape examination

Fracture shape was examined using Scanning Electron Microscopy (SEM) with an accelerating voltage of 15 kV and 1000x-magnification. Samples for SEM were cut, mounted in epoxy resin, ground, and polished using 1- μ m diamond particles. After polishing, the samples were coated with Iridium prior to SEM examination.

**Fig. 4** Locations of mechanical test samples in a coupon

4 Results and discussion

4.1 Mechanical behavior assessment

4.1.1 Tensile strength

ANOVA showed that UTS is not affected by the electrode diameter ($p > 0.1$), while it is significantly affected by the deposition angle ($F_{23,3} = 5.04$, $p = 0.012$). Specifically, UTS in longitudinal direction decreases when the deposition angle is in the range from 0 to 30° reaching its lowest value at deposition angle of 30°. A remarkable increase in UTS (~34.6% in some coupons) was observed when the deposition angle was 45° compared to deposition angle of 0°, as indicated in Fig. 5.

Moreover, cup and cone fracture shape was strongly dominant for all specimens made using angles of deposition of 0°, 15°, and 30° with the exception of one specimen per each angle. In the samples built with 45° deposition angle, an inclined fracture line was dominant among all the testing coupons except for one specimen of those made with the smaller electrode diameter (Table 3). It is noted that the 45° deposition angle resulted in coupons with UTS of 417 MPa on average, which is very close to that of

the original electrode material. It is worth mentioning that the measured UTS of the electrodes was about 420 MPa on average.

More importantly, regarding anisotropic behavior, UTS did not statistically differ between longitudinal and transverse directions in the testing coupons built with deposition angles of 30° and 45° ($p > 0.1$). In contrast, coupons built with 0° and 15° angles showed statistically lower UTS values ($p < 0.01$) in the longitudinal direction than in the transverse direction. Thus, coupons built with angles 0° and 15° are considered anisotropic; some of these coupons had UTS in the longitudinal direction about 30% less than in the transverse direction.

4.2 Toughness

ANOVA results revealed that there was no significant effect of angle and electrode diameter (and their interactions) on toughness ($p > 0.1$), see Figs. 6, 7. Further, toughness did not statistically differ between longitudinal and transverse directions in the testing coupons built with deposition angles of 30° and 45° ($p > 0.1$), indicating more isotropic behavior of testing coupons. In contrast, toughness was statistically lower ($p < 0.05$) in the longitudinal direction compared to transverse direction for deposition angles of 0° or 15°. Thus, coupons built with angles 0° and 15° are statistically considered anisotropic with respect to toughness. Some of these coupons showed toughness in the longitudinal direction that is as much as 44% less than that in the transverse direction (Fig. 6).

Nevertheless, toughness variation trend was seen to oppose that noticed in UTS across the angles. For those samples cut in the transverse direction, higher toughness was noticed at deposition angles of zero and 15° when compared to those at 45° (Fig. 6). A possible justification for these observations can be that the parts built with angles less than 45° are under bending at layer level and that the lower the angle, the higher the effect of bending and the less the effect of the shear stress [38]. On the other hand, the higher values of toughness at 15° compared to zero angle can be linked to the fact that the ends of layers deposited at 15° are interlocked by the ends of the opposing layers deposited at -15°. This is unlike the layers deposited at zero angle where there is a higher possibility of poor bonding at layer ends.

4.3 Number of layers/beads

The number of layers is of interest in this study because it affects the part's building time as well as its mechanical behavior. ANOVA results showed that the number of deposited layers was significantly influenced by both electrode diameter and layer inclination angle, as well as their interaction ($F_{23,1} = 102.8$, $p < 0.01$), ($F_{23,3} = 137.26$,

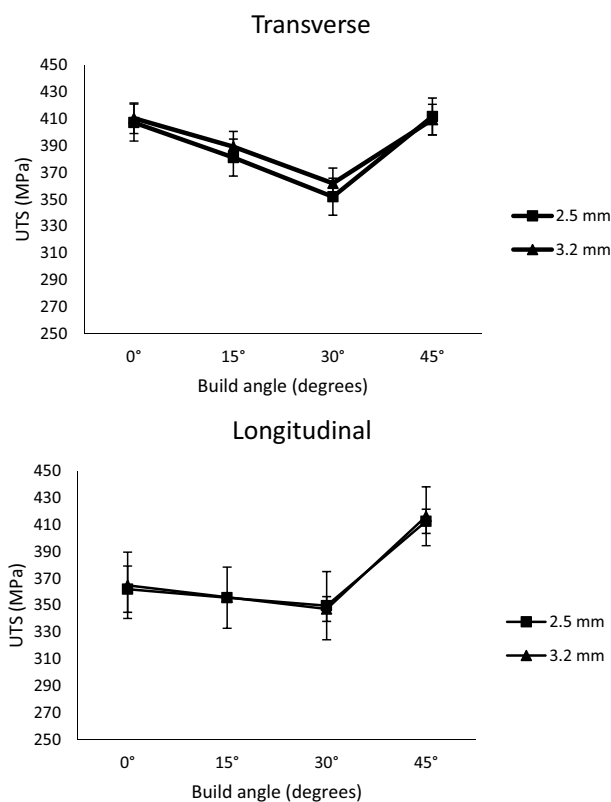







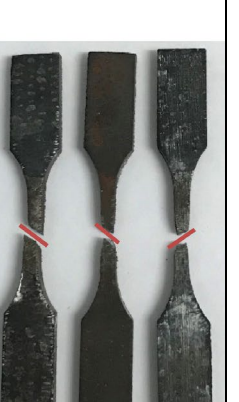


Fig. 5 Effect of build angle, electrode diameter on UTS

Table 3 Samples of tensile fracture shape

Electrode Diameter	Angle			
	0°	15°	30°	45°
2.5 mm				
3.2 mm				

$p < 0.01$), and ($F_{23,3} = 12.16$, $p < 0.01$), respectively. As Fig. 8 shows, the 3.2-mm diameter electrode deposits 44 layers, compared to 64 layers by the 2.5-mm one, to build the same part height. On the other hand, the number of layers increases with the deposition angle because shorter layers are deposited with each stroke when the substrate surface is inclined with respect to the deposition direction.

It is worth noting that Pearson correlation test revealed a positive correlation between number of layers and UTS ($r = 0.455$, $p = 0.026$). Thus, the larger the number of layers, the higher is the UTS expected from coupons deposited at 45°. Also, more layers in one orientation means more layers in the opposite orientation, which results in higher impedance to deformation and yielding under the applied load.

4.4 Scanning electron microscopic examination

Samples for examination of fracture morphology using scanning electron microscope were obtained from each testing coupon. ASTM standard procedure was followed for samples preparation and images capturing using SEM. Samples of tensile fracture images for each test condition are shown in Fig. 9. Basically, dimples dominated fracture surface for those samples made at angles 15° and 0°. Many voids with different sizes were also noticed in fracture surface for samples fabricated at angles of 15° and 0°. These observations suggest that those sample failed from layers bending under applied load during tensile testing (voids dominant fracture mechanism), which explains the dominance of cup and cone shape of fracture among

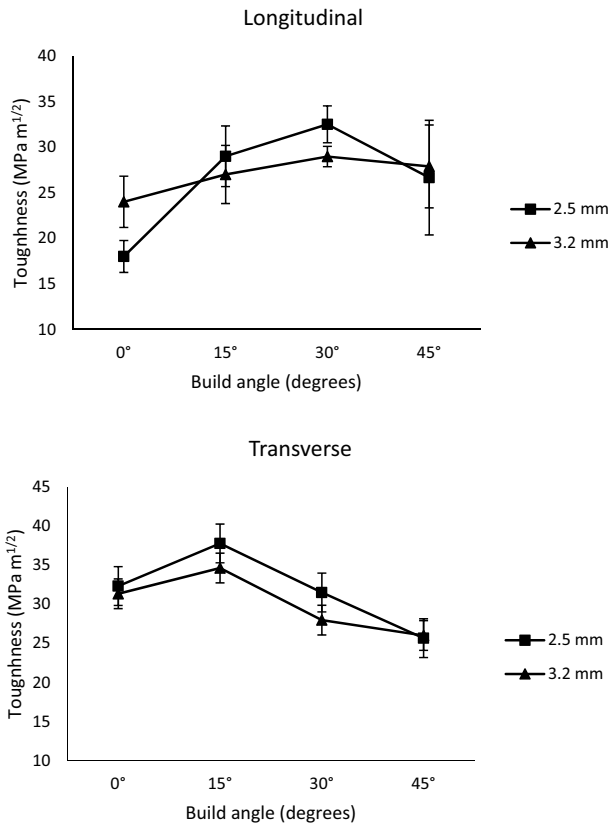


Fig. 6 Effect of build angles and electrode diameter on toughness

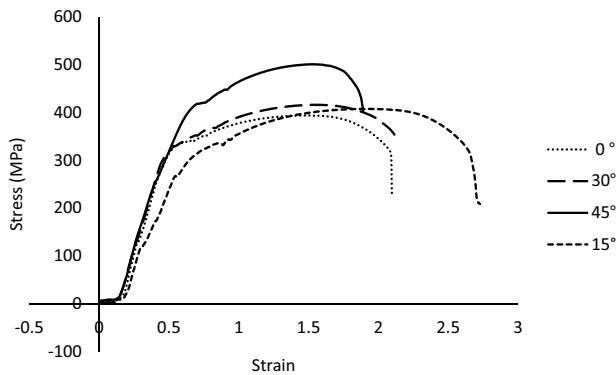


Fig. 7 Stress–strain curve at different deposition angles

all of them. In other words, when layers were deposited horizontally, the layers were basically under dominance of bending during tensile testing unlike other deposition angles where layers experienced both bending and shear stress. As angle changes, the bending and shear stress components change too, thus fracture results from interplay between the voids dominant fracture and shear-slip fracture. It is worth noting that few shear bands can be

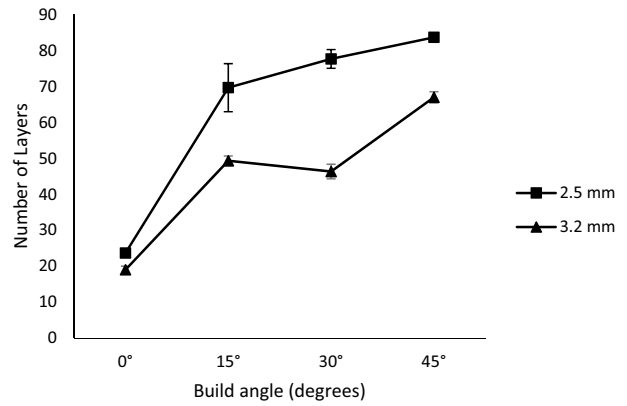


Fig. 8 Effect of build angle, electrode diameter on number of layers

found on fracture surface of samples made at 15°, which justifies tensile strength reduction compared to those at 0°.

In contrast, shear bands dominated the samples built at 45°. This suggests shear failure among those samples and justifies the higher tensile strength as well as lower elongation values of testing coupons built using this angle. Fracture morphology for samples made at angle 30° shows combinations of shear bands, voids, and dimples. However, minor voids and fewer dimples were noticed, suggesting that samples were both under bending and shear stress, which explains their lower tensile strength compared to samples at angles 0° and 15°.

5 Conclusions

This work proposed a new layer deposition technique based on varying the deposition angle with respect to XZ-plane and tested it using AWS E6013 low carbon steel electrodes. The deposition technique was found capable of reducing the anisotropic behavior and hence improving functionality of AM parts. Using a deposition angle of 45° and a 3.2-mm diameter electrode helped retain the original electrode material’s strength. This experimental study had certain limitations related to the available resources. The limited electrode length caused weld discontinuity in some cases when it is fully consumed during a layer deposition. Moreover, some of the test coupons experienced significant bending distortions due to shrinking after deposition. Therefore, future work should focus on mitigating these issues, in addition to testing more electrode sizes and deposition angle combinations. In particular, a combination of 0° and 45° deposition angles within the same part could give a better or similar strength with a shorter building time than what was achieved in this study. Also, more testing on the effect of the proposed technique on hardness and grain size is of interest for future work.

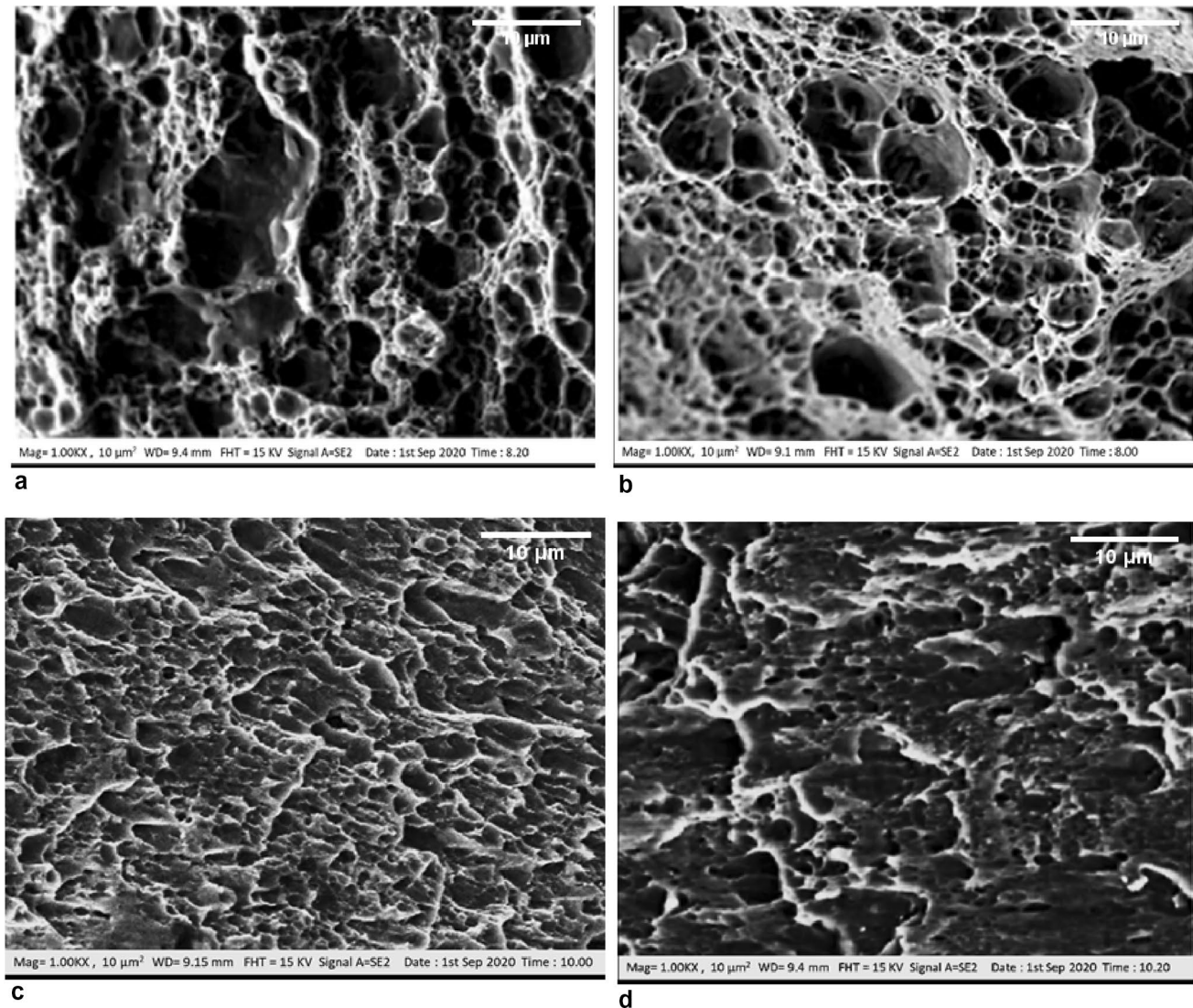


Fig. 9 SEM images at the center region for tensile fracture morphology **a** 0°, **b** 15°, **c** 30° and **d** 45°. Fracture SEM images obtained at 1000× with scale for all images 10 μm

Acknowledgements The authors would like to thank the Engineering Workshops and Deanship of Research at Jordan University of Science and Technology for their help throughout this work.

Funding This research did not receive any specific grant from funding agencies in the public, commercial, or not-for-profit sectors.

Declarations

Conflict of interest On behalf of all authors, the corresponding author states that there is no conflict of interest.

References

1. Frazier WE (2014) Metal additive manufacturing: a review. *J Mater Eng Perform* 23:1917–1928
2. Paskual A, Álvarez P, Suárez A (2018) Study on arc welding processes for high deposition rate additive manufacturing. *Procedia Cirp* 68:358–362
3. Cyr E, Lloyd A, Mohammadi M (2018) Tension-compression asymmetry of additively manufactured Maraging steel. *J Manuf Process* 35:289–294

4. Mellor S, Hao L, Zhang D (2014) Additive manufacturing: a framework for implementation. *Int J Prod Econ* 149:194–201
5. Cunningham CR, Flynn JM, Shokrani A, Dhokia V, Newman ST (2018) Invited review article: strategies and processes for high quality wire arc additive manufacturing. *Addit Manuf* 22:672–686
6. Youheng F, Guilan W, Haiou Z, Liye L (2017) Optimization of surface appearance for wire and arc additive manufacturing of Bainite steel. *Int J Adv Manuf Technol* 91:301–313
7. Yehorov Y, da Silva LJ, Scotti A (2019) Exploring the use of switchback for mitigating homoepitaxial unidirectional grain growth and porosity in WAAM of aluminium alloys. *Int J Adv Manuf Technol* 104:1581–1592
8. Sun R, Li L, Zhu Y, Guo W, Peng P, Cong B, Sun J, Che Z, Li B, Guo C (2018) Microstructure, residual stress and tensile properties control of wire-arc additive manufactured 2319 aluminum alloy with laser shock peening. *J Alloys Compd* 747:255–265
9. Xu X, Ganguly S, Ding J, Dirisu P, Martina F, Liu X, Williams SW (2019) Improving mechanical properties of wire + arc additively manufactured maraging steel through plastic deformation enhanced aging response. *Mater Sci Eng A Struct Mater* 747:111–118
10. Colegrove PA, Donoghue J, Martina F, Gu J, Prangnell P, Hönnige J (2017) Application of bulk deformation methods for microstructural and material property improvement and residual stress and distortion control in additively manufactured components. *Scr Mater* 135:111–118
11. Williams SW, Martina F, Addison AC, Ding J, Pardal G, Colegrove P (2016) Wire + Arc additive manufacturing. *Mater Sci Technol (United Kingdom)* 32(7):641–647
12. Geng H, Li J, Xiong J, Lin X, Zhang F (2017) Geometric limitation and tensile properties of wire and arc additive manufacturing 5A06 aluminum alloy parts. *J Mater Eng Perform* 26:621–629
13. Wang L, Xue J, Wang Q (2019) Correlation between arc mode, microstructure, and mechanical properties during wire arc additive manufacturing of 316L stainless steel. *Mater Sci Eng A* 751:183–190
14. Zhang C, Li Y, Gao M, Zeng X (2018) Wire arc additive manufacturing of Al-6Mg alloy using variable polarity cold metal transfer arc as power source. *Mater Sci Eng A* 711:415–423
15. Zhu Y, Tian X, Li J, Wang H (2015) The anisotropy of laser melting deposition additive manufacturing Ti-6.5 Al-3.5 Mo-1.5 Zr-0.3 Si titanium alloy. *Mater Des* 67:538–542
16. Zhang Q, Chen J, Zhao Z, Tan H, Lin X, Huang W (2016) Microstructure and anisotropic tensile behavior of laser additive manufactured TC21 titanium alloy. *Mater Sci Eng A* 673:204–212
17. Caballero A, Ding J, Ganguly S, Williams S (2019) Wire + Arc Additive Manufacture of 17-4 PH stainless steel: effect of different processing conditions on microstructure, hardness, and tensile strength. *J Mater Process Technol* 268:54–62
18. Shen C, Mu G, Hua X, Li F, Luo D, Ji X, Zhang C (2019) Influences of postproduction heat treatments on the material anisotropy of nickel-aluminum bronze fabricated using wire-arc additive manufacturing process. *Int J Adv Manuf Technol* 103:3199–3209
19. Thompson MK et al (2016) Design for Additive Manufacturing: trends, opportunities, considerations, and constraints. *CIRP Ann Manuf Technol* 65(2):737–760
20. Nancharaiyah T (2011) Optimization of process parameters in FDM process using design of experiments. *Int J Emerg Technol* 2(1):100–102
21. Taufik M, Jain PK (2016) A study of build edge profile for prediction of surface roughness in fused deposition modeling. *J Manuf Sci Eng*. <https://doi.org/10.1115/1.4032193>
22. Vahabli E, Rahmati S (2017) Improvement of FDM parts' surface quality using optimized neural networks—medical case studies. *Rapid Prototyp. J.* 23(4):825–842
23. Nuñez PJ, Rivas A, García-Plaza E, Beamud E, Sanz-Lobera A (2015) Dimensional and surface texture characterization in fused deposition modelling (FDM) with ABS plus. *Procedia Eng* 132:856–863
24. Garg PK, Singh R, Ahuja IPS (2017) Multi-objective optimization of dimensional accuracy, surface roughness and hardness of hybrid investment cast components. *Rapid Prototyp J* 23(5):845–857
25. Khoshkhoo A, Carrano AL, Blersch DM (2018) Effect of surface slope and build orientation on surface finish and dimensional accuracy in material jetting processes. *Procedia Manuf.* 26:720–730
26. Klinga JH, Dahmen CG, Baier T, Mohanty S, Hattel JH (2019) Build orientation effects on the roughness of SLM channels. In: In joint special interest group meeting between euspen and ASPE advancing precision in additive manufacturing, pp. 111–114
27. Fatimatuzahraa AW, Farahaina B, Yusoff WAY (2011) The effect of employing different raster orientations on the mechanical properties and microstructure of Fused Deposition Modeling parts. In: ISBEIA 2011–2011 IEEE Symposium on Business, Engineering and Industrial Applications, pp 22–27
28. Armillotta A, Carcallaro M (2017) Edge quality in fused deposition modeling: I. Definition and analysis. *Rapid Prototyp J* 23(6):1079–1087
29. Hill N, Haghi M (2014) Deposition direction-dependent failure criteria for fused deposition modeling polycarbonate. *Rapid Prototyp J.* 20(3):221–227
30. Domingo-Espin GR, Puigoriol-Forcada JM, Garcia-Granada AA, Lluma J, Borros S (2015) Mechanical property characterization and simulation of fused deposition modeling Polycarbonate parts. *Mater Des* 83:670–677
31. Cantrell JT, Rohde S, Damiani D, Gurnani R, DiSandro L, Anton J, Young A, Jerez A, Steinbach D, Kroese C (2017) Experimental characterization of the mechanical properties of 3D-printed ABS and polycarbonate parts." *Rapid Prototyp. J.* 23(4):811–824
32. Deng X, Zeng Z, Peng B, Yan S, Ke W (2018) Mechanical properties optimization of poly-ether-ether-ketone via fused deposition modeling. *Materials (Basel)* 11(2):216
33. Afrose MF, Masood SH, Iovenitti P, Nikzad M, Sbarski I (2016) Effects of part build orientations on fatigue behaviour of FDM-processed PLA material. *Prog Addit Manuf* 1(1–2):21–28
34. Keleş Ö, Blevins CW, Bowman KJ (2017) Effect of build orientation on the mechanical reliability of 3D printed ABS. *Rapid Prototyp J* 23(2):320–328
35. Crocchio D, De Agostinis M, Fini S, Olmi G, Vranic A, Ciric-Kostic S (2016) Influence of the build orientation on the fatigue strength of EOS maraging steel produced by additive metal machine. *Fatigue Fract Eng Mater Struct* 39(5):637–647
36. Bogojević S, Ćirić-Kostić A, Vranic G, Olmi G, Crocchio D (2020) Influence of the orientation of steel parts produced by DMLS on the fatigue behavior. In: *Lecture Notes in Mechanical Engineering*, pp 294–305
37. Karlsson P, Pejryd L, Oikonomou C (2017) Factors influencing mechanical properties of additive manufactured thin-walled parts. In: *Proceedings Euro PM 2017: international powder metallurgy congress and exhibition*
38. Mortazavian S, Fatemi A (2015) Effects of fiber orientation and anisotropy on tensile strength and elastic modulus of short fiber reinforced polymer composites. *Compos Part B Eng* 72:116–129

Publisher's Note Springer Nature remains neutral with regard to jurisdictional claims in published maps and institutional affiliations.